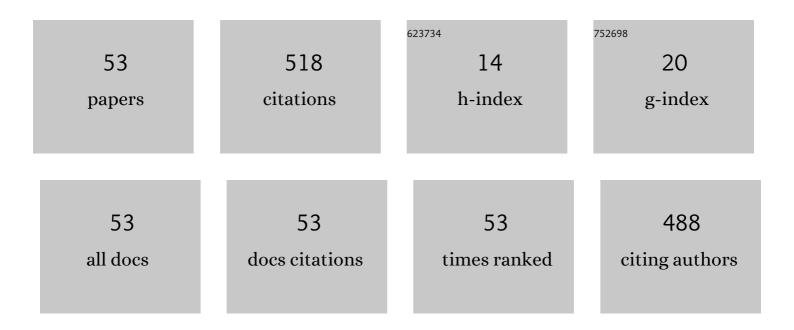
Chong-Hun Jung

List of Publications by Year in descending order

Source: https://exaly.com/author-pdf/342784/publications.pdf Version: 2024-02-01



#	Article	IF	CITATIONS
1	Title is missing!. Journal of Radioanalytical and Nuclear Chemistry, 2000, 246, 299-307.	1.5	59
2	Electrosorption of uranium ions on activated carbon fibers. Journal of Radioanalytical and Nuclear Chemistry, 2011, 287, 833-839.	1.5	44
3	Effect of surface modification of silica nanoparticles by silane coupling agent on decontamination foam stability. Annals of Nuclear Energy, 2018, 114, 11-18.	1.8	29
4	The surface modification and characterization of SiO2 nanoparticles for higher foam stability. Scientific Reports, 2020, 10, 19399.	3.3	25
5	Adsorption of rhenium and rhodium in nitric acid solution by Amberlite XAD-4 impregnated with Aliquat 336. Korean Journal of Chemical Engineering, 2006, 23, 303-308.	2.7	21
6	Hybrid of Graphene based on quaternary Cu2ZnNiSe4 –WO3 Nanorods for Counter Electrode in Dye-sensitized Solar Cell Application. Scientific Reports, 2020, 10, 4738.	3.3	21
7	Ion exchange characteristics of palladium from nitric acid solution by anion exchangers. Korean Journal of Chemical Engineering, 1999, 16, 571-575.	2.7	19
8	Effect of silica nanoparticles on the stability of decontamination foam and their application for oxide dissolution of corroded specimens. Annals of Nuclear Energy, 2014, 73, 168-174.	1.8	18
9	New Design of Active Material Based on YInWO ₄ -G-SiO ₂ for a Urea Sensor and High Performance for Nonenzymatic Electrical Sensitivity. ACS Biomaterials Science and Engineering, 2020, 6, 6981-6994.	5.2	17
10	Polypyrrole-Bonded Quaternary Semiconductor LiCuMo ₂ O ₁₁ –Graphene Nanocomposite for a Narrow Band Gap Energy Effect and Its Gas-Sensing Performance. ACS Omega, 2020, 5, 17337-17346.	3.5	17
11	New design of mesoporous SiO2 combined In2O3-graphene semiconductor nanocomposite for highly effective and selective gas detection. Journal of Materials Science, 2020, 55, 13085-13101.	3.7	17
12	Photocatalytic activities of contaminants by Bi2WO6-graphene composites decorated with mesoporous silica. Journal of Alloys and Compounds, 2018, 766, 477-487.	5.5	16
13	Stabilizing decontamination foam using surface-modified silica nanoparticles containing chemical reagent: foam stability, structures, and dispersion properties. RSC Advances, 2021, 11, 1841-1849.	3.6	16
14	Preparation of PAN-zeolite 4A composite ion exchanger and its uptake behavior for Sr and Cs ions in acid solution. Korean Journal of Chemical Engineering, 2002, 19, 838-842.	2.7	14
15	Sonochemical synthesis of quaternary LaNiSbWO4-G-PANI polymer nanocomposite for photocatalytic degradation of Safranin-O and gallic acid under visible light irradiation. Journal of Photochemistry and Photobiology A: Chemistry, 2020, 394, 112484.	3.9	14
16	Highly efficient visible light driven photocatalytic activities of the LaCuS2-graphene composite-decorated ordered mesoporous silica. Separation and Purification Technology, 2018, 205, 11-21.	7.9	13
17	Analysis of Combustion Kinetics of Powdered Nuclear Graphite by using a Non-isothermal Thermogravimetric Method. Journal of Nuclear Science and Technology, 2006, 43, 1436-1439.	1.3	12
18	Cold Plasma Processing and Plasma Chemistry of Metallic Cobalt Surface. Plasma Chemistry and Plasma Processing, 2008, 28, 617-628.	2.4	12

CHONG-HUN JUNG

#	Article	IF	CITATIONS
19	3D Modeling of Silver Doped ZrO2 Coupled Graphene-Based Mesoporous Silica Quaternary Nanocomposite for a Nonenzymatic Glucose Sensing Effects. Nanomaterials, 2022, 12, 193.	4.1	12
20	The double perovskite structure effect of a novel La2CuNiO6-ZnSe-graphene nanocatalytic composite for dye sensitized solar cells as a freestanding counter electrode. Photochemical and Photobiological Sciences, 2019, 18, 1389-1397.	2.9	11
21	Highly enhanced foams for stability and decontamination efficiency with a fluorosurfactant, silica nanoparticles, and Ce(IV) in radiological application. Environmental Technology and Innovation, 2020, 18, 100744.	6.1	11
22	Separation of Palladium from a Simulated Radioactive Liquid Waste by Precipitation Using Ascorbic Acid. Separation Science and Technology, 2000, 35, 411-420.	2.5	9
23	Structure and stability of decontamination foam in concentrated nitric acid and silica nanoparticles by image analysis. Annals of Nuclear Energy, 2016, 95, 102-108.	1.8	9
24	The Application of Visualization and Simulation in a Dismantling Process. Journal of Nuclear Science and Technology, 2007, 44, 649-656.	1.3	8
25	Synergetic effect of La2CdSnTiO4-WSe2 perovskite structured nanoparticles on graphene oxide for high efficiency of dye sensitized solar cells. Journal of Alloys and Compounds, 2019, 775, 690-697.	5.5	7
26	Photocatalytic activities using a nanocomposite of mesoporous SiO2 and CdInSe-graphene nanoparticles under visible light irradiation. Journal of Photochemistry and Photobiology A: Chemistry, 2019, 371, 271-281.	3.9	7
27	New modeling of AgFeNi2S4-graphene-TiO2 ternary nanocomposite with chelate compounds and its photocatalytic reduction of CO2. Journal of Materials Science: Materials in Electronics, 2021, 32, 9804-9821.	2.2	7
28	Three-dimensional of graphene oxide Ba2VPbSe6 framework composite attach on cellulose based counter electrode for dye-sensitized solar cell. Journal of Photochemistry and Photobiology A: Chemistry, 2019, 372, 11-20.	3.9	6
29	Non-enzymatic sensing of glucose with high specificity and sensitivity based on high surface area mesoporous BiZnSbV-G-SiO2. Journal of Materials Science: Materials in Electronics, 2021, 32, 8330-8346.	2.2	6
30	New modeling of 3D quaternary type BaCuZnS-graphene-TiO2 (BCZS-G-T) composite for photosonocatalytic hydrogen evolution with scavenger effect. Photochemical and Photobiological Sciences, 2020, 19, 1765-1775.	2.9	6
31	Adsorptive separation of rhenium and rhodium in nitric acid solution using a column packed with an extractant impregnated resin. Korean Journal of Chemical Engineering, 2006, 23, 1023-1027.	2.7	5
32	Morphological Control of Mesoporous Silica Nanoparticles and Their Application for Foam Stability. Asian Journal of Chemistry, 2014, 26, 1401-1404.	0.3	5
33	Novel designed quaternary CuZnSnSe semiconductor combined graphene-polymer (CuZnSnSe-C-PPy) composites for highly selective gas-sensing properties. Journal of Materials Science: Materials in Electronics, 2021, 32, 12812-12821.	2.2	5
34	A comparative study on the laser removal of Cs+ ion from type 304 stainless steel. Korean Journal of Chemical Engineering, 2010, 27, 1780-1785.	2.7	4
35	Development of the In-situ Monitoring System for Pipe Internal Contamination Measurement in the Decommissioning Site. Journal of Nuclear Science and Technology, 2008, 45, 500-502.	1.3	3
36	Modification of graphene based on a Ba2Cu8Ni2Se12 catalyst with CoS nanospheres for a counter electrode for dye-sensitized solar cells. New Journal of Chemistry, 2020, 44, 4199-4205.	2.8	3

CHONG-HUN JUNG

#	Article	IF	CITATIONS
37	Size distribution and filtration property of particles generated from laser ablation decontamination process. Environmental Progress and Sustainable Energy, 2013, 32, 649-654.	2.3	2
38	3D ternary LaCdSe-GO-TiO2 nanocomposite synthesized with high powersonic method and sonophotocatalytic efficiency for hydrogen evolution with different scavengers. Research on Chemical Intermediates, 2021, 47, 3411-3436.	2.7	2
39	The Application of Visualization and Simulation in a Dismantling Process. Journal of Nuclear Science and Technology, 2007, 44, 649-656.	1.3	2
40	Melting Decontamination of Radioactive Scrap Metal by Graphite Arc Melter. Journal of Chemical Engineering of Japan, 2008, 41, 607-611.	0.6	1
41	The effect of NO 3 â^' and OHâ^' ions on the laser ablation of Cs+ ion on Type 304 stainless steel. Journal of Radioanalytical and Nuclear Chemistry, 2011, 287, 525-531.	1.5	1
42	Distribution of the Radionuclides during the Melting of Aluminum Wastes Generated from the TRIGA MARK III Research Reactor. Journal of Chemical Engineering of Japan, 2008, 41, 602-606.	0.6	1
43	Analysis of Combustion Kinetics of Powdered Nuclear Graphite by using a Non-isothermal Thermogravimetric Method. Journal of Nuclear Science and Technology, 2006, 43, 1436-1439.	1.3	1
44	Separation of Technetium in Nitric Acid Solution With an Extractant Impregnated Resin. , 2006, , 527.		0
45	Characteristics of Melting for the Radioactive Aluminum Wastes From the Decommissioned Nuclear Facilities. , 2006, , 475.		0
46	Development and Performance Assessment of a Soil Washing Equipment for Soil Contaminated With Radionuclide. , 2007, , 965.		0
47	Characteristics of a nuclides distribution during a melt decontamination of radioactive aluminum wastes. Korean Journal of Chemical Engineering, 2008, 25, 1344-1349.	2.7	0
48	Decontamination of Metal Surfaces Artificially Contaminated With Cs+ Ions by a Laser Ablation. , 2009, , .		0
49	Sorption of cobalt by amine-functionalized silica nanoparticles for foam decontamination of nuclear facilities. Journal of Radioanalytical and Nuclear Chemistry, 2016, 310, 841-847.	1.5	0
50	The viability of rumpled La2CrFeW6-CdSe perovskite wrapped by graphene for a viable efficiency and icreased utilization of dye-sensitized solar cells. Materials Technology, 2019, 34, 247-257.	3.0	0
51	Metal Surface Decontamination by the PFC Solution. , 2006, , .		0
52	ICONE15-10596 CHARACTERISTICS OF URANIUM DISTRIBUTION DURING THE METAL MELTING IN AN ELECTRIC ARC FURNACE. The Proceedings of the International Conference on Nuclear Engineering (ICONE), 2007, 2007.15, _ICONE1510ICONE1510.	0.0	0
53	The Technical Development for Reuse of Radioactive Concrete Waste Generated by Dismantling of Nuclear Facilities. , 2008, , .		0